Paper 069

WIND TUNNEL CORRECTIONS FOR ISOLATED ROTOR TESTS

M. Biava[1], M. Valentini[2], L. Vigevano[2]

[1] AWPARC, Milano, Italy [2] Dipartimento di Scienze e Tecnologie Aerospaziali - Politecnico di Milano, Via La Masa 34, 20156 Milano, Italy

Abstract

A coupled CFD/CSD method has been employed to simulate both a model rotor in the open test section of the Politecnico di Milano large wind tunnel and a geometrically similar full-scale rotor in free air. The trimmed rotor is represented by a steady actuator disk model. Keeping constant the trim target in terms of thrust coefficient and flapping angles, the rotor performance have been matched by varying the shaft angle. The comparison between the results relative to the two different environments and geometric scales led to the definition of a shaft angle correction procedure, that permits to correlate the wind tunnel measurements to the performance of the real rotor in free flight.

1 Introduction

It is well known that when performing helicopter rotor tests in a wind tunnel we have induced velocities in the near field of the rotor which are not the same as in free-air. Apart from the geometric scale effects, the different inflow velocity distribution leads to a variation of the rotor performance: for instance, if the net effect of the wind tunnel environment is to produce an additional upwash at the rotor disk (this is the typical effect of a closed test section), the measured torque will be lower than the free-air value, since in the experiment the rotor blades will experience (in average) a higher angle of attack for the same collective control angle; on the contrary, if the net effect is an additional downwash (typical of open test sections), the measured torque will be higher than in free-air. The magnitude of this performance variation depends on the dimensions of the wind tunnel test section relative to the model rotor, on the shape of the test section, etc.

In addition, closed test section experiments at low tunnel speed and high thrust operating conditions may present a so called *flow breakdown*, when the interaction between the rotor wake and the tunnel walls strongly modify the flow in the vicinity of the rotor due to the onset of recirculation[1–6], thus making the use of wall corrections inadequate.

In open sections, *flow breakdown* occurrence is less evident. The nature of the interference between tunnel jet and rotor wake is substantially different than that experienced in closed sections and also much less known. To qualitatively investigate the model rotor behavior in such conditions, a campaign of experimental measurements and numerical simulations was carried out in the $4 \times 3.8\,\mathrm{m}$ open test section of the Politecnico di Milano (PoliMi) large wind tunnel using a model rotor, kindly provided by AgustaWestland (AW)[7]. The computations were performed with the Navier-Stokes solver *ROSITA*[8,9]. The rotor effects were represented with an Actuator Disk (AD) model with non uniform assigned load. The tunnel and rotor operating parameters range were identified, where a strong interaction between rotor wake and the deflectors of the divergent portion of the tunnel could occur. A practical means to detect these critical conditions during the actual wind tunnel operations was also given, based on pressure measurements at some selected loca-

tions of the lower deflector.

This preliminary investigation was not sufficient, however, to determine quantitative wall correction measures, because the AD model was not trimmed to feel the interference effects. The need of simulating the rotor in wind tunnel experimental conditions, where a specific trim state is reached manually, required the development of a coupled aerodynamic/structural (CFD/CSD) method able to reproduce numerically the trimmed state. Due to the high computational cost of coupled CFD/CSD full-rotor simulations, a method based on an AD model of the rotor coupled with the *MBDyn* multi-body software[10] has been conceived[11], which is able to simulate a rotor in steady trim state at a fraction of the cost of a full-rotor simulation. Despite the relatively small requirements in terms of computational resources, the method proved to be accurate when tested against available experimental data[11].

The coupled CFD/CSD method has been employed to simulate both the AW model rotor in the open test section and a geometrically similar full-scale rotor in free air. Keeping constant the trim target in terms of thrust coefficient and flapping angles, the rotor performance have been matched by varying the shaft angle, so that the comparison between the results relative to the two different environments and geometric scales led to the definition of a shaft angle correction procedure, that permits to correlate the wind tunnel measurements to the performance of the real rotor in free flight.

The structure of this paper is as follows. Section 2 summarizes the results of the set of numerical simulations, carried out in the wind tunnel environment and in free flight with the coupled CFD/CSD method. Some details of the numerical parameters are given, together with the calibration procedure to determine the tunnel velocity. Section 3 describes the shaft angle correction procedure and reports the achieved results. Some conclusions are drawn in the last section.

2 Actuator disk trimmed simulations

Details of the CFD solver *ROSITA*[8,9], multi-body solver *MBDyn*[10] and coupled CFD/CSD AD model[11] are given elsewhere and will not be repeated here. This section will first describe the procedure needed to numerically reproduce the reference flow speed read on the Wind Tunnel (WT) instrumentation display. The numerical calibration curve is used to assign a wind tunnel velocity to each of the simulations of the rotor in the open test section in a way that is consistent with the experiments. Then the results of the numerical simulations, performed in wind tunnel and in free-air conditions and needed to devise the wall corrections, will be presented.

2.1 Numerical wind tunnel calibration

The flow speed reported by the wind tunnel instrumentation display is not measured directly during the wind tunnel operation. Instead, the static pressure in two points of the tunnel convergent portion, at different distances from the exit section, is recorded (see figure 1). The pressure difference ΔP between the two points is related to the displayed WT speed V_{wt} by means of a calibration curve. This curve is obtained prior to the actual model tests by measuring the air speed at the center of the test section (with empty tunnel) by means of a Pitot tube at different WT power settings. From the above explanation it is clear that, when operating the wind tunnel for rotor tests, the displayed speed is *not* the actual flow speed in the test section center, but the speed that there would be in the test section center of the *empty* tunnel operating at the same value of ΔP.

In order to have a similar definition of the wind tunnel velocity for the CFD computations, we reproduced numerically the previously described calibration procedure. A series of CFD simulations of the empty tunnel have been performed, and the value of ΔP between the measuring points indicated in figure 1 has been extracted from the computed flow fields. The resulting V_{wt}-ΔP curve is plotted in figure 2 and it is compared with the calibration curve of the real wind tunnel, measured experimentally. The two curves are in good agreement for low flow speed, while at higher speeds the CFD velocity in the section center is lower than the corresponding measured one. This discrepancy may be explained by a lack of geometrical details of the simulations. The actual wind tunnel mounts a series of aerodynamic de-

vices at the nozzle exit to damp flow oscillations that caused resonance phenomena. These devices, that are not represented in the CFD simulations, have also the effect of thickening the shear layer of the jet exiting the nozzle and, consequently, of reducing the cross sectional area of the potential core of the jet; this area reduction is the cause of the higher flow speed found in the experimental calibration curve.
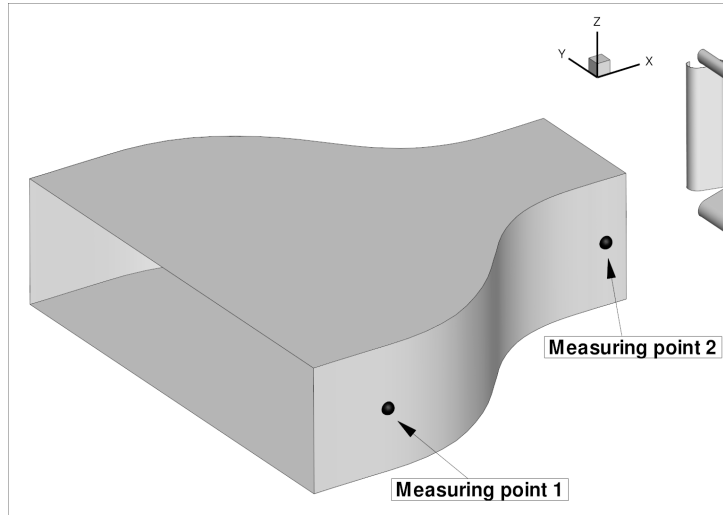

Figure 1: Position of the pressure probes used for determining the displayed flow speed.
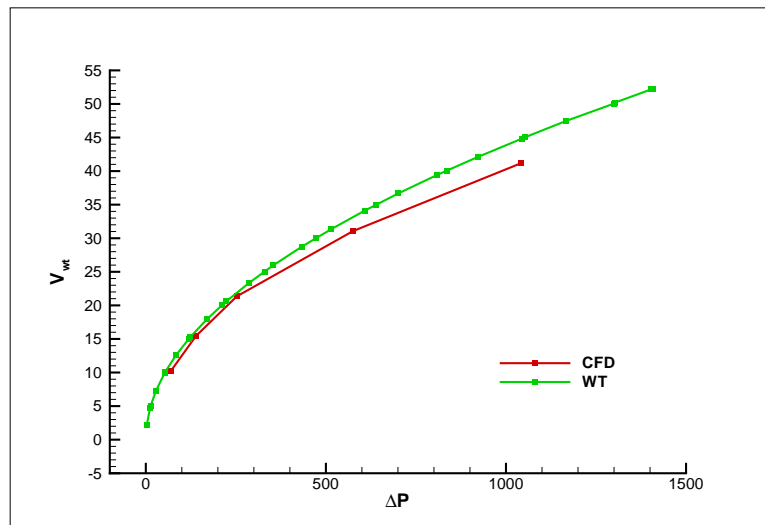

Figure 2: Experimental and numerical wind tunnel velocity calibration curve.

2.2 Open test section simulations

In the present section we describe the numerical simulations of the trimmed model rotor in the open test section of the Politecnico di Milano large wind tunnel. The simulations were performed us-ing the coupled actuator disk method described in Biava *et al.*[11].

Figure 3 shows the numerical domain used for the simulations. The Chimera grid system consists of the following components: a background mesh
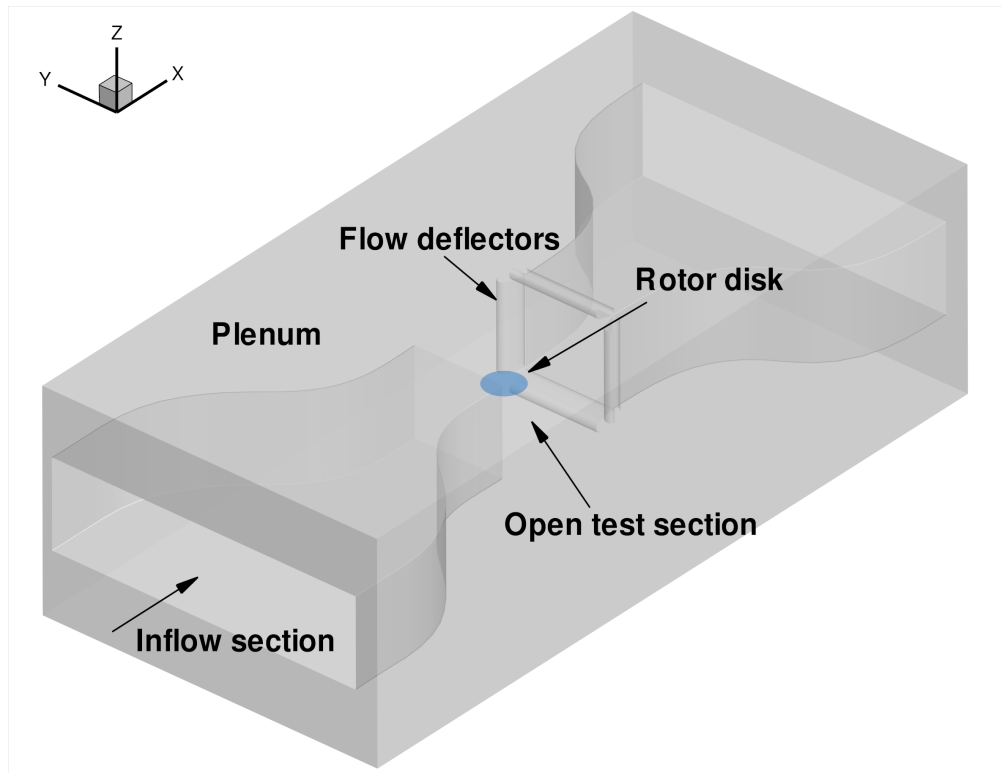
Figure 3: Numerical domain for the CFD computations.
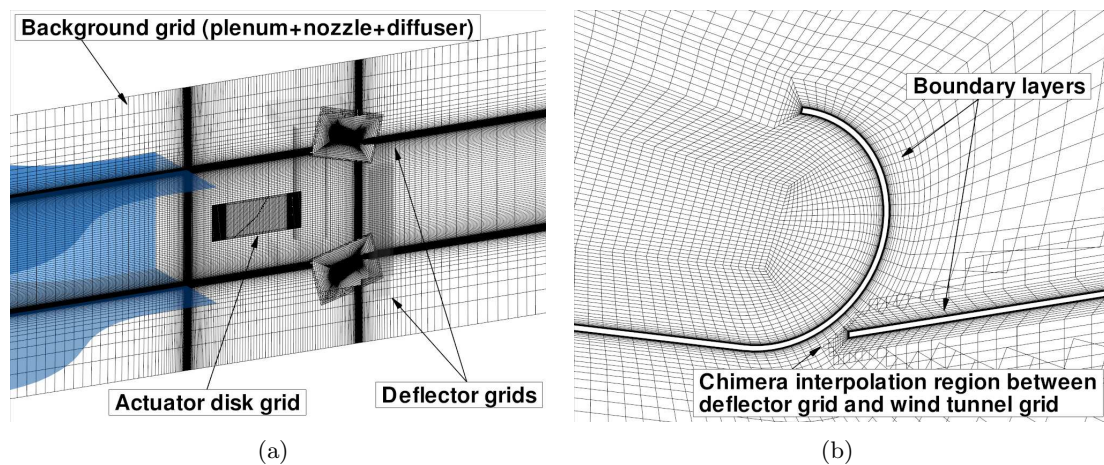

(a)

(b)

Figure 4: A slice of the computational grid in the symmetry plane of the wind tunnel (a) and a zoomed view of the slice close to the upper deflector (b).

which represents the chamber containing part of the wind tunnel circuit and the open test section – the shape of the wind tunnel and the dimensions of the surrounding chamber were directly taken from a 3D CAD of the wind tunnel; four grids representing the flow deflectors placed at the beginning of the wind tunnel return circuit; a cylindrical mesh

for the actuator disk.

The figure 4 reports a slice of the computational mesh in the symmetry plane of the wind tunnel, where the different component grids can be clearly viewed. A magnified view of the mesh close to the upper deflector is also shown in the same figure to make clear the cell distribution in
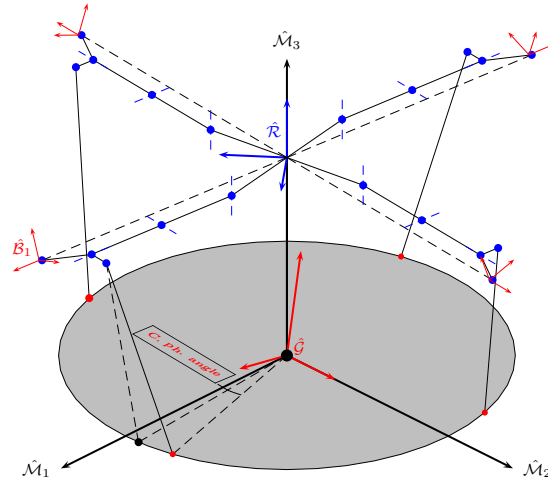
Figure 5: *MBDyn* model of the 4-bladed rotor hub.

the region of Chimera interpolation between the deflector grid and the wind tunnel grid. It can also be noted that the solid walls (deflectors and wind tunnel walls) have non-zero thickness. In total the mesh contains about 13 million cells. The applied boundary conditions are: viscous wall boundary conditions on the wind tunnel walls; inviscid wall boundary conditions on the chamber walls; velocity inlet boundary conditions at the inflow section; pressure outlet boundary conditions at the outflow section.

The employed *MBDyn* model (figure 5) defines the 4-bladed AW model rotor, implementing a high fidelity reproduction of the whole rotor kinematics, including the complete articulation mechanism of the hinges and pitch links. Several reference systems are utilized to represent the model components, as indicated in figure 5: the fixed inertial frame $\hat{\mathcal{G}}$, the shaft frame $\hat{\mathcal{M}}$, the rotating frame $\hat{\mathcal{R}}$ and the local blade frame $\hat{\mathcal{B}}$.

The aerodynamic C81 tables for the blade airfoils, to be used in the Blade Element Theory (BET) of the trimmed AD model, were computed for an average value of the Re/M (Reynolds over Mach) of 2×10^6, in order to represent the model-scale rotor.

The simulation of the model rotor in the open test section environment revealed itself to be a challenging task, due to the low speed working range of the tunnel and the need of simulating at the same time the fluid nearly at rest occupying the chamber surrounding the test section jet. To achieve accurate results in this low Mach number condition necessitated the use of a preconditioner for the finite volume formulation of the Navier–Stokes compressible equations in *ROSITA*. A Turkel type preconditioner[12] was selected and proved to be effective for the CFD simulations of the wind tunnel flow, both in terms of convergence and accuracy.

For all the presented simulations the *ROSITA* solver was run in parallel on 72 processors. The simulations took 5 to 10 *ROSITA*/*MBDyn* coupling cycles to converge, depending on the operating conditions, but it generally takes longer for low wind speeds. At each coupling cycle *ROSITA* was run performing 2000 pseudo-time iterations at CFL=2.0 when $V_{\mathrm{wt}} = 10\,\mathrm{m/s}$ and at CFL=5.0 for all the other speeds; the cycle computational time was 10 hours (wall clock). The time consumed by *MBDyn* at each cycle is roughly 5 minutes and it is therefore negligible.

The parameter extracted from the simulations that is of interest for the purpose of determining the wall corrections is the torque coefficient C_q as a function of the wind tunnel speed V_{wt}. In figure 6 the normalized C_q-V_{wt} curve for the simulations performed at $C_T/\sigma = 0.1$ is compared with the corresponding experimental results.
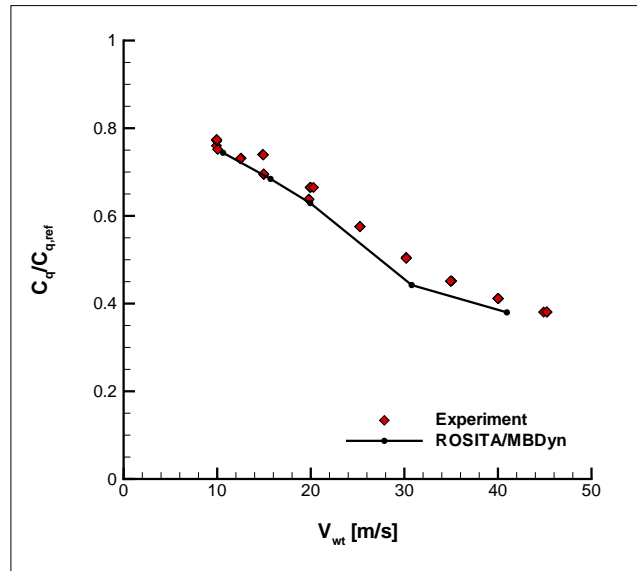
Figure 6: Computed and experimental values of the normalized torque coefficient for $C_T/\sigma = 0.1$
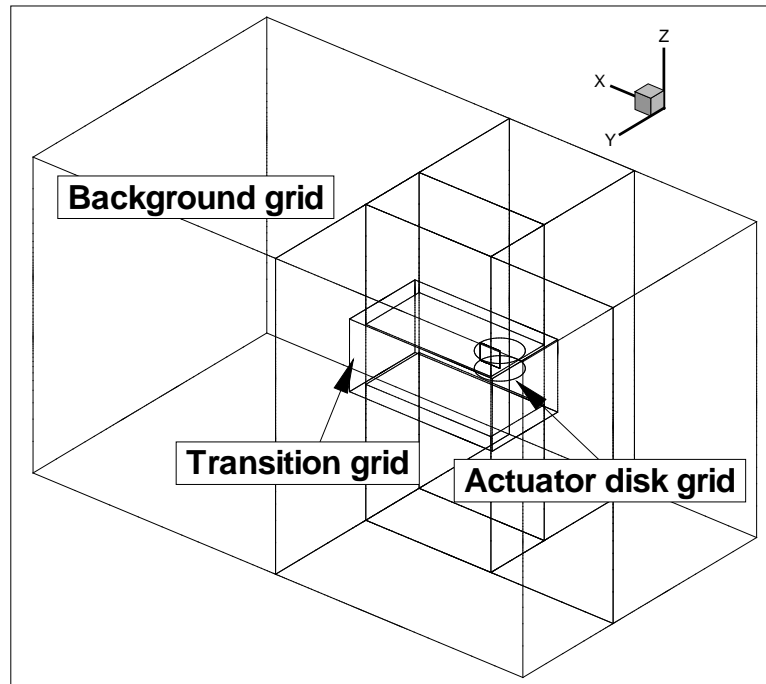

Figure 7: Numerical domain for the free-air CFD computations.

2.3 Free air simulations

Figure 7 shows the numerical domain used for the simulations. The Chimera grid system consists in this case of three components: a background mesh which extends up to the far-field; a transition grid, with intermediate density, to better capture the rotor wake; a cylindrical mesh for the actuator disk.

The employed *MBDyn* model is that shown in figure 5 but scaled to full-scale dimensions. The aerodynamic C81 tables for the blade airfoils were now computed for an average value of the Re/M
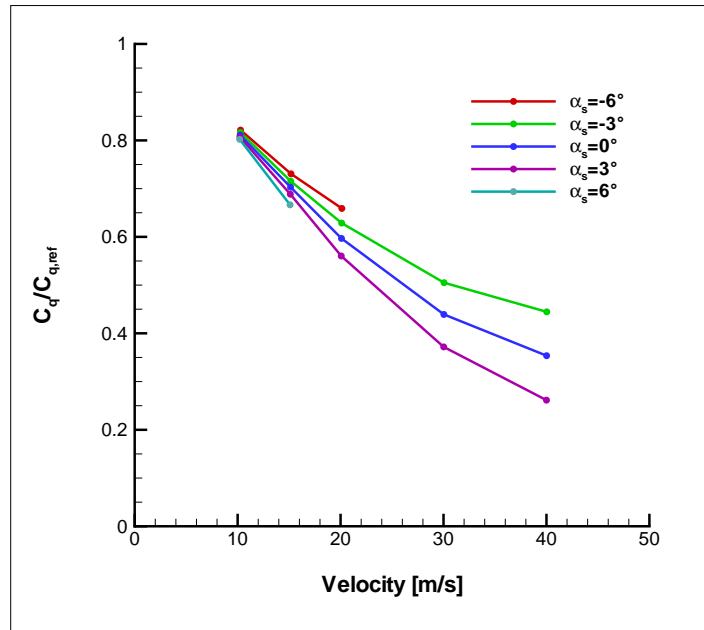
Figure 8: Computed values of the normalized torque coefficient for $C_T/\sigma = 0.1$ and various shaft angles.
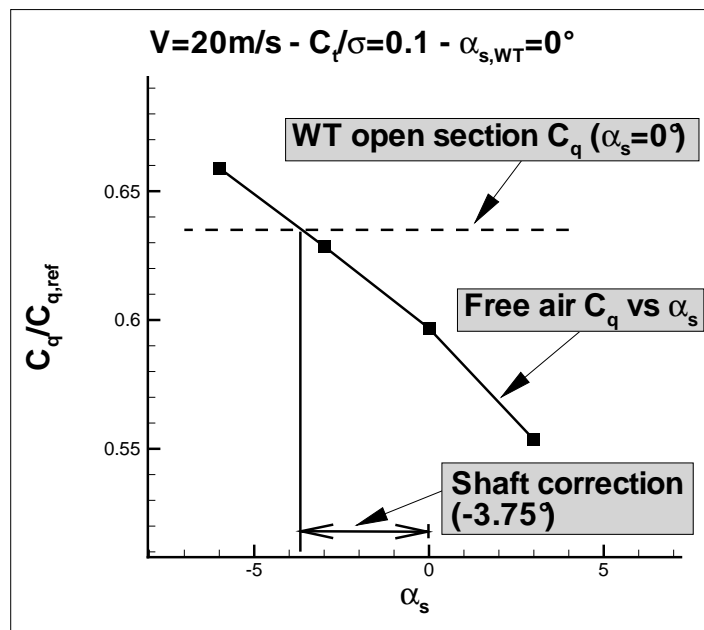

Figure 9: Example of shaft correction.

(Reynolds over Mach) of 14×10^6, in order to represent the full-scale rotor and account for Reynolds number effects.

The numerical parameters and computational characteristics of the simulations are similar to those described for the WT simulations, but for the computational efficiency which is higher for the free air simulations. For instance, the cycle computational time was now just 2 hours (wall clock). The considered combinations of wind tunnel flow speed and rotor thrust coefficient cover the range $10 < V_\infty < 40\,\mathrm{m/s}$, $0.08 < C_T/\sigma < 0.12$. The steady simulations have been performed with the RANS solver using the Spalart-Allmaras

turbulence model.

The improved efficiency with respect to the wind tunnel calculations allowed to simulate several shaft angle configurations with acceptable turnaround time. This procedure proved to be much more convenient than fixing a reference free-air condition and varying the shaft angle of the model rotor in the wind tunnel to match the torque coefficient. The normalized C_q-V_{wt} curves for $C_T/\sigma = 0.1$ and different shaft angles in free-air are shown in figure 8. We recall that the shaft angle is assumed negative nose down. As expected, the higher is the shaft angle (with sign) the lower is the required torque.

3 Correction procedure

The comparison between the results relative to the two different environments and geometric scales leads to the definition of a correction procedure, that permits to correlate the wind tunnel measurements to the performance of the real rotor in free flight.

We start from the observation that varying the shaft angle of a rotor has the main effect of inducing an additional downwash or upwash at the rotor disk. The former case happens if we reduce the shaft angle (*i.e.* helicopter nose down) and the latter if we increase the shaft angle. It is thus possible to translate the influence of the wind tunnel environment as a variation of the shaft angle of the rotor: if a test rotor in the wind tunnel, in a specific flight condition and shaft angle $\alpha_{s,wt}$, has a torque coefficient $C_{q,wt}$, the same rotor in free-flight shall have the same torque coefficient at a different shaft angle $\alpha_{s,free}$, keeping fixed all the other conditions. The difference $\Delta\alpha_s = \alpha_{s,free} - \alpha_{s,wt}$ may be defined as the "shaft angle correction".

The above definition is better explained with a specific example. We consider a rotor tested in the wind tunnel with the following flight condition: $C_T/\sigma = 0.1$, $\beta_{1,s} = 0$ and $\beta_{1,c} = 0$ (tip path plane normal to the shaft), $V_{wt} = 20\,\text{m/s}$, $\alpha_{s,wt} = 0°$. The measured normalized torque coefficient turns out to be $C_{q,wt} = 0.635$. Now suppose that we are able to measure the normalized torque coefficient $C_{q,free}$ experienced by the same rotor in free-flight, in the same flight conditions

and at the same shaft angle: due to the wall interference effects in the wind tunnel it will likely happens that $C_{q,wt} \neq C_{q,free}$. It is then possible to vary the shaft angle of the rotor in free-air, keeping fixed the other parameters, until we find the angle $\alpha_{s,free} = -3.75°$ at which $C_{q,wt} = C_{q,free}$ and we finally define the correction for this specific condition as $\Delta\alpha_s = -3.75° - 0° = -3.75°$. The situation is illustrated in figure 9.

Starting from the achieved numerical results and following the procedure outlined above, it is possible to define the shaft corrections for the Politecnico di Milano large wind tunnel with open test section. The numerical results were obtained for the 4-bladed AW rotor, but the obtained correction values are equally applicable for any rotor having the same size, since the specific features of the rotor, like blade shape and number of blades have lesser influence on the corrections.

In figure 10(a) we have reported, for example, the computed torque coefficient in the wind tunnel and in the free-air environment for $C_T/\sigma = 0.1$ as function of the flow speed. The colored curves refer to the full-scale rotor in free-air at different shaft angles, the blue curve being that for $\alpha_{s,free} = 0\circ$; the black curve refers instead to the model-scale rotor in the wind tunnel with open test section. The black curve lies above the blue for $V_{wt} = 16.8\text{-}40\,\text{m/s}$: in this velocity range the shaft correction is *negative*, that is, in free-air we have to put the rotor "more nose down" to have the same shaft torque as in the wind tunnel; the magnitude of the corrections is relatively small: $|\Delta\alpha_s| < 3.75°$ (see figure 10(b)). For $V_{wt} < 16.8\,\text{m/s}$ the sign of the correction changes, and the magnitude tends to increase rapidly as the WT velocity decreases. Actually, at $V_{wt} = 10\,\text{m/s}$ the normalized $C_{q,free}$ covers a small range of values for all shaft angles and the $C_{q,wt}$ lies outside of this range: therefore the shaft correction is evaluated by extrapolation, thus explaining its large value.

We reported in Table 1 the shaft corrections for all the computed flight conditions. Note again that for $V_{wt} = 10\,\text{m/s}$ the rotor flow is very strongly influenced by the wind tunnel walls interference and the shaft correction has to be extrapolated. The corrections for intermediate conditions may be derived by interpolation.

C_T/σ	$V = 10$m/s	$V = 15$m/s	$V = 20$m/s	$V = 30$m/s	$V = 40$m/s
0.08	12.58° [*]		-0.41°	-3.46°	-3.37°
0.10	38.00° [*]	2.15°	-2.97°	-0.76°	-1.06°
0.12	168.58° [*]		-6.38°	-3.24°	-2.75°

Table 1: Shaft angle corrections for the Politecnico di Milano large wind tunnel open section. The value with the (∗) superscript has been extrapolated.
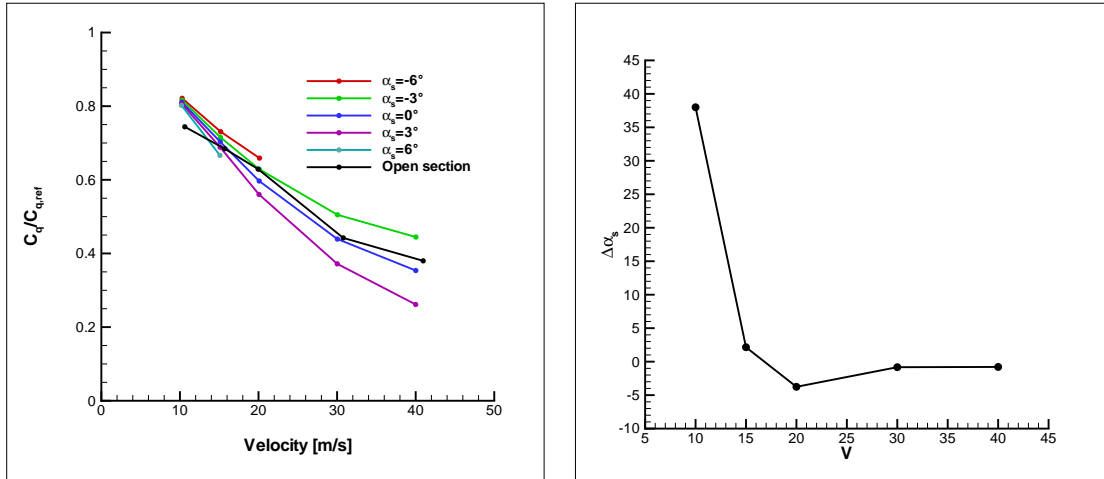

Figure 10: Computed values of the normalized torque coefficient in wind tunnel and free-air environment for $C_T/\sigma = 0.1$ (left) and computed shaft corrections for $C_T/\sigma = 0.1$ (right).

This result is consistent with the qualitative numerical analysis of the flow in the open test section performed by Biava *et al.*[7], where for $V_\text{wt} < 20$ m/s the rotor wake either escapes almost completely the wind tunnel return circuit or strongly impacts on the lower deflector (figure 11). In these operating conditions the tunnel jet is significantly bent downwards and a ground effect due to the interaction between the wake and the deflector occurs. Therefore, in such conditions the distortion of the flow introduced by the wind tunnel walls is too strong for the measured performance to be correlated to the free-air values. It follows that the rotor tests performed at Politecnico di Milano large wind tunnel may be correlated to the corresponding full-scale rotor flight in free-air only when $V_\text{wt} > 20$ m/s. For the lower velocities the wind tunnel tests may be used only for rotor-to-rotor comparisons.

We conclude by comparing the computed corrections with those given by the classical Glauert theory (see Langer[4]), that expresses the shaft angle correction by means of the following formula:

$$\Delta\alpha_\text{s} = \frac{180}{\pi}\frac{2\delta_\text{wt}C_T A}{\mu^2 A_\text{wt}}, \qquad (1)$$

where μ is the advance ratio, A is the rotor disk aerea, A_wt is the test section aerea and δ_wt is a correction coefficient specific to the wind tunnel, which is typically negative for open test sections and positive for closed test sections. The normalization factor $180/\pi$ that appears in the right hand side of equation (1) is needed to convert $\Delta\alpha_\text{s}$ to degrees since δ_wt is customarily given in radians.

Solving equation (1) for δ_wt and inserting the computed $\Delta\alpha_\text{s}$, we obtain the values of δ_wt given in Table 2. If we keep into account only the velocities above 20 m/s, the range where we consider the corrections to be meaningfully applicable, we see that the coefficient δ_wt is roughly constant and negative, as it is expected for a wind tunnel with open test section.
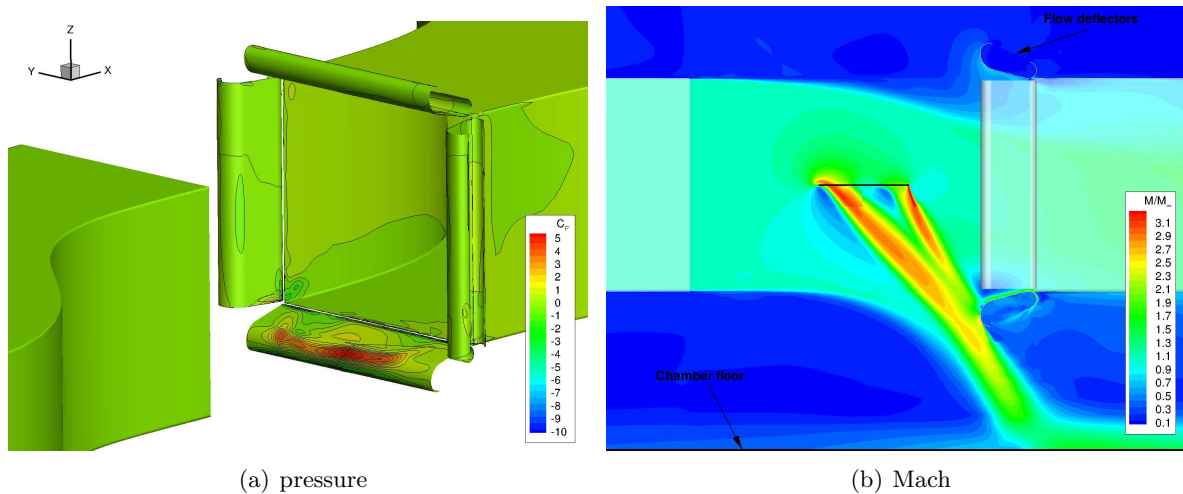
(a) pressure

(b) Mach

Figure 11: Pressure coefficient distribution on the tunnel walls (left) and Mach number distribution in the vertical symmetry plane of the test section (right) for $V_\infty = 10\,\text{m/s}$, $C_T/\sigma = 0.10$, from [7].

C_T/σ	$V = 10\text{m/s}$	$V = 15\text{m/s}$	$V = 20\text{m/s}$	$V = 30\text{m/s}$	$V = 40\text{m/s}$
0.08	0.14		-0.02	-0.34	-0.59
0.10	0.33	0.04	-0.10	-0.06	-0.15
0.12	1.23		-0.19	-0.21	-0.32

Table 2: Value of the correction coefficient δ_wt in the Glauert formula for the Politecnico di Milano large wind tunnel open section.

4   Conclusions

The main outcome of the present work is the definition of shaft angle correction coefficients for the PoliMi large wind tunnel with open section, so as to predict with accuracy the performance of full-scale rotors in free-air flight starting from measurements on model rotors. The achievement of this result, notwithstanding the required large effort in CFD and multi-body dynamic modeling, allows a better understanding of the wall interference effects and a precise definition of the set of wind tunnel operating conditions where the experiment is representative of free-air rotor flow. For the specific case of the PoliMi large wind tunnel open section, this turned out to be feasible for $V_\text{wt} > 20\,\text{m/s}$. Within this bounds the wall corrections are applicable; instead, out of these working conditions, the rotor testing is still possible but should be limited to rotor-to-rotor comparisons. This increased knowledge gives the experimentalist more confidence in the wind tunnel operation and in the interpretation of the measurements.

Aknowledgements: this work has been carried out in the framework of Project WITCH (WInd Tunnel Correction metHodology for model rotor tests), funded by AWPARC.

Copyright Statement

References

[1] W.H. Rae Jr. Limits on Minimum-Speed V/STOL Wind-Tunnel Tests. *Journal of Aircraft*, 4(3):249–254, 1967.

[2] F.D. Harris. Aerodynamic and Dynamic Ro-

tary Wing Model Testing in Wind Tunnels and Other Facilities. In *AGARD LS 63 "Helicopter Aerodynamics and Dynamics"*, 1973.

[3] J.-J. Philippe. Consideration on wind-tunnel testing techniques for rotorcrafts. In *AGARD Special Course on Aerodynamics of Rotorcraft*, 1990.

[4] H.J. Langer, R.L. Peterson, and T.H. Maier. An Experimental Evaluation of Wind Tunnel Wall Correction Methods for Helicopter Performance. In *American Helicopter Society 52nd Annual Forum Proceedings*, 1996. Washington, DC.

[5] P. M. Shinoda. Wall interaction effects for a full-scale helicopter rotor in the NASA Ames 80- by 120-foot wind tunnel. In *AGARD Meeting on "Wall Intereference, Support Interference and Flow Field Measurements"*, 1993.

[6] M. Biava, A. Thomopoulos, and L. Vigevano. Computational assessment of flow breakdown in closed section model rotor tests. In 37th *European Rotorcraft Forum, Vergiate/Gallarate, Italy*, 2011.

[7] M. Biava, G. Campanardi, G. Gibertini, D. Grassi, L. Vigevano, and A. Zanotti. Wind tunnel open section characterization for rotorcraft tests. In 38th *European Rotorcraft Forum, Amsterdam, The Netherlands*, 2012.

[8] M. Biava. *RANS computations of rotor/fuselage unsteady interactional aerodynamics.* PhD thesis, Dipartimento di Ingegneria Aerospaziale, Politecnico di Milano, 2007.

[9] M. Biava, W. Khier, and L. Vigevano. CFD prediction of air flow past a full helicopter configuration. *Aero. Sci. Tech.*, 19:3–18, 2012.

[10] Mbdyn - multibody dynamics http://www.aero.polimi.it/mbdyn/.

[11] M. Biava, M. Valentini, and L. Vigevano. Trimmed Actuator Disk Modeling for Helicopter Rotor. In 39th *European Rotorcraft Forum, Moscow, Russia, paper 94*, 2013.

[12] E. Turkel, R. Radespiel, and N. Kroll. Assessment of preconditioning methods for multidimensional aerodynamics. *Computers & Fluids*, 6:613–634, 1997.